京都大学防災研究所年報 第 56 号 B 平成 25 年 6 月
Annuals of Disas. Prev. Res. Inst., Kyoto Univ., No. 56 B, 2013

Influence of a Series of Sabo Dams on Debris Flow Deposition

Namgyun Kim(1), Hajime NAKAGAWA, Kenji KAWAIKE and Hao ZHANG

(1) Graduate School of Engineering, Kyoto University

Synopsis

Since ancient times, debris flow has been recorded. It is a kind of mixture flow of water and sediment. It causes damage of human's lives and properties. Large boulders in the front of surge and big destructive force are common for debris flow. To mitigate debris flow disaster, various kinds of sabo dams have been constructed. Control function of such sabo dams have been reported through a lot of studies. However there are still few studies about combination of sabo dam. In this study, experimental and numerical works have been performed for influencing on capture capacity of sabo dam by upper located sabo dam. Results indicate that depending on the conditions of arrangement of sabo dam can affect the storage capacity.

Keywords: debris flow, sabo dam, distance, deposition, potential storage volume

1. Introduction

Debris flows are found in mountainous environment, which consist of fully saturated mixtures of water, sediment, debris. Debris flows are widely recognized as one of the geomorphic processes in steep mountainous area. (Takahashi et al., 1992; Hunger et al., 2001; Vandine et al., 2002) Debris flows initiated high on the slope of hill and it increased in volume by entraining material from the channels. It flows down a slope under gravitational force. Furthermore, the mass of debris are transported downstream and debris flow disaster spreads in residential area(Fig. 1). The effects of debris flows can cause morphological change, serious casualties and damage to properties due to large boulders are in front of wave. Debris flow disasters have been occurred in East Asia. Fig. 2 shows the number of occurrence of debris flow in Japan. The debris flows occur annually. Therefore, structural countermeasures have been designed to preserve humans and their properties are constructed in order to prevent debris flows.

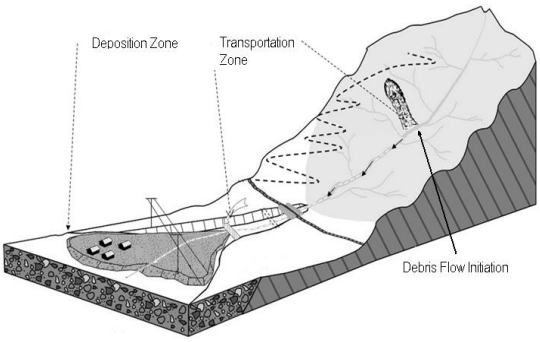

Fig. 1 Stages of debris flow (Takahashi, 1992)

Countermeasures can be classified as structural and non-structural measures. In the structural measures, sabo dams are one of the effective structural countermeasures to control the debris flow. Sabo dams, which are often constructed in series, have been used in East Asia and Europe to mitigate the debris flow hazard. Fig. 3 shows a closed-type sabo dam constructed to mitigate

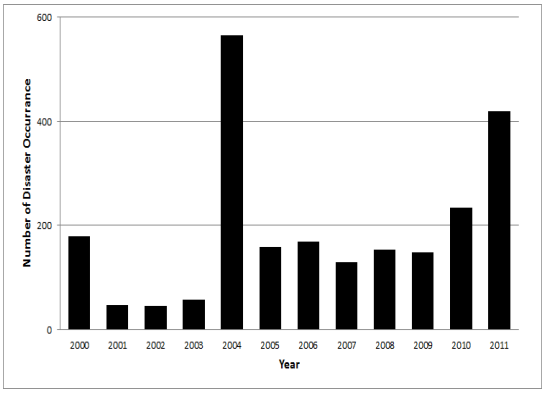

Fig. 2 The number of debris flow occurrence in Japan

Fig. 3 Closed-type sabo dam

debris flow in downstream area. Sabo dams are designed to control sediment volume, sediment size and hydrograph of debris flow. Such functions of sabo dams are described in many experimental and computational studies(Honda et al., 1997; Imran, J. et al., 2001). Also, considerable theoretical and numerical works have been performed on the size, shape and structure of torrential Sabo dams (Mizuyama et al., 1988; Johnson et al., 1989). Takahashi et al. proposed a method to take into account the effect of a closed-type sabo dam. These studies have contributed to technical guidelines related to debris flows. However, further studies are needed to develop general guidelines of sabo dam. Understanding the processes that debris flow deposition upstream of a sabo dam is important for the design Sabo dams.

This study is focused on the optimal distance of each closed-type sabo dam. It is conducted experiments and simulation to propose optimal distance of each closed-type sabo dam. The fundamental one dimensional depth averaged model is used. The deposition velocity equations proposed by Shrestha et al. is chosen for deposition process upstream of a sabo dam.

2. Laboratory experiments

The laboratory experiments were carried out using rectangular flume of 4.7m long, 20cm high, 10cm wide. The slopes of flume is set $18°$. The details of the experimental setup are shown in fig. 4. A sediment bed of silica sand and gravel mixtures sediment with 1.5m long and 10cm deep was positioned 3m to 4.5m upstream measured from the outlet of the flume. This laid sediment bed is saturated by water as seepage flow. Sediment materials with mean diameter $d_m = 2.86mm$, maximum diameter $d_{max} = 15mm$ and density $\sigma = 2.65\mathrm{g/cm^3}$ were used. Fig. 5 shows particle

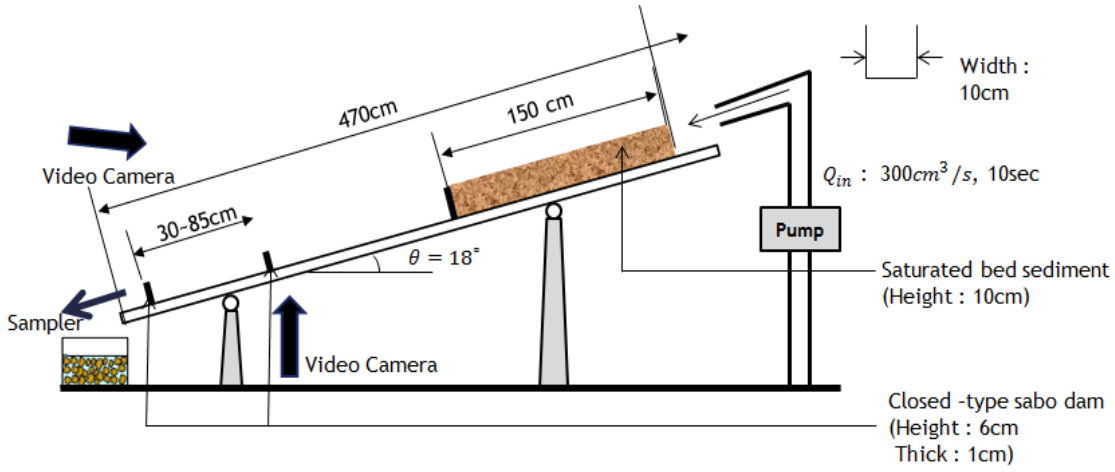

Fig. 4 Experimental flume set up

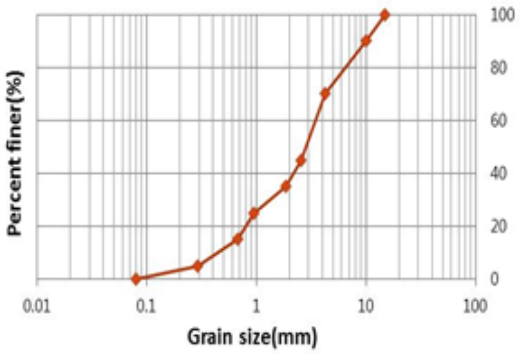

Fig. 5 Particle size distribution of sediment materials

Table 1 Experimental condition

Experiment No.	Supply water Discharge (cm^3/s)	Time (sec)	Distance of each dam (cm)
Case.A-1	300	10	30
Case.A-2		10	55
Case.A-3		10	80
Case.B-1		20	30
Case.B-2		20	55
Case.B-3		20	80

size distribution. Two closed-type sabo dams were used for this study. One sabo dam was set at 450cm from upstream end of flume. The other sabo dam was set at 420cm, 395cm and 365cm from upstream end of flume. Sabo dams of 6cm high, 1cm thickness were used.

The experimental conditions are shown in Table 1. Debris flow was generated by supplying a constant water discharge $300cm^3/sec$ for 10sec from the upstream end of the flume. Debris flow produced in the experiments is the fully stony type debris flow and the largest particles were accumulated in the forefront. Using two standard video cameras, debris flow deposition patterns upstream of each sabo dam were captured. Also, debris flow captured volume of each sabo dam was measured.

3. Numerical model

3.1 Spacing between sabo dams

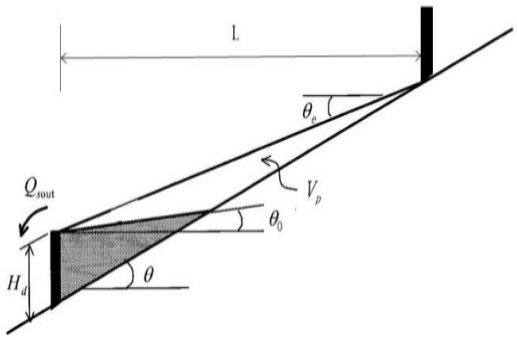

Fig. 6 Schematics of closed-type sabo dam

As shown in Fig. 6, the spacing between sabo dams depends on stream gradient, dam height, angle of deposition of material behind the dam. Chatwin et al. provides a formula for the spacing of sabo dams:

$$L > \frac{H_d}{\tan(\theta-\theta_e)} \quad (1)$$

where H_d is the height of dam, θ is original channel gradient, θ_e is the equilibrium bed slope.

Minimum spacing between dams is determined by captured volume of sabo dam. Since the evaluation of the control function of sabo dams is based on the assumption that Ssbo dams are initially filled with sediment up to crest level, estimation of the sediment volume trapped by each sabo dam is carried out based on the potential storage volume (V_p) of each dam, which can be defined by equilibrium and initial bed deposition slopes. V_p is described as follows.

$$V_p = \frac{(H_d\, cos\theta)^2 B}{2}\left\{\frac{1}{\tan(\theta-\theta_e)} - \frac{1}{\tan(\theta-\theta_0)}\right\} \quad (2)$$

where, H_d height of dam, B is the flow width, $\theta_0$is the initial bed slope of storage area before occurring debris flow.

3.2 Governing equations

Debris flow is described using one dimensional depth averaged equations. The equations for the mass conservation of water-sediment mixture (3) and only sediment (4) can be described as following equations.

$$\frac{\partial h}{\partial t}+\frac{\partial M}{\partial x}=i \tag{3}$$

$$\frac{\partial (Ch)}{\partial t}+\frac{\partial (CM)}{\partial x}=iC_* \tag{4}$$

The equations for momentum conservation are as follow;

$$\frac{\partial M}{\partial t}+\beta\frac{\partial (uM)}{\partial x}=gh\sin\theta_b-gh\cos\theta_b\frac{\partial h}{\partial x}-\frac{\tau_b}{\rho_T} \tag{5}$$

where M (=uh) is flow flux in x direction, u is mean velocity, h is flow depth, i erosion (>0)or deposition (≤ 0) velocity, C is the sediment concentration in the flow, C_* is maximum sediment concentration in the bed, β is momentum correction factor equal to 1.25 for a stony debris flow, g is the acceleration due to gravity, τ_b is bottom shear stress, ρ_T is mixture density ($\rho_T=\sigma C+(1-C)\rho$) , σ is density of the sediment particle, ρ is density of the water.

The equation of bed variation is described as follows:

$$\frac{\partial z_b}{\partial t}+i_b=0 \tag{6}$$

where z_b is erosion or deposition thickness of the bed measured from the original bed surface elevation, i_b is bed erosion or deposition velocity.

The erosion and deposition velocity have been given by Takahashi et al. are described as follows.

Erosion velocity, if $C<C_\infty$;

$$i=\delta\frac{C_\infty-C}{C_*-C_\infty}\frac{M}{d_m} \tag{7}$$

Deposition velocity, if $C\geq C_\infty$;

$$i=\delta'\frac{C_\infty-C}{C_*}\frac{M}{d_m} \tag{8}$$

where δ is erosion coefficient, δ' is deposition coefficient, $d_m$is mean diameter of sediment, C_∞ is the equilibrium sediment concentration described as follows(Nakagawa et al.,2003):

If $tan\theta_w$ >0.138, a stony type debris flow occurs, and

$$C_\infty=\frac{\rho_m\tan\theta_w}{(\sigma-\rho_m)(\tan\phi-\tan\theta_w)} \tag{9}$$

If 0.03< $tan\theta_w\leq 0.138$, an immature type debris flow occurs, and

$$C_\infty=6.7\left\{\frac{\rho_m\tan\theta_w}{(\sigma-\rho_m)(\tan\phi-\tan\theta_w)}\right\}^2 \tag{10}$$

If $tan\theta_w\leq 0.03$, a turbulent water flow with bed load transport occurs, and

$$C_\infty=\frac{(1+5\tan\theta_w)\tan\theta_w}{\sigma/\rho_m-1}\left(1-\alpha_0^2\frac{\tau_{*c}}{\tau_*}\right)\left(1-\alpha_0^2\sqrt{\frac{\tau_{*c}}{\tau_*}}\right) \tag{11}$$

where $\theta_w$is water surface gradient, ρ_m is density of the interstitial muddy fluid, ϕ is internal friction angle of the sediment, and

$$\alpha_0^2=\frac{2\{0.425-(\sigma/\rho_T)\tan\theta_w/(\sigma/\rho_T-1)\}}{1-(\sigma/\rho_T)\tan\theta_w/(\sigma/\rho_T-1)} \tag{12}$$

$$\tau_{*c}=0.04\times 10^{1.72\tan\theta_w} \tag{13}$$

$$\tau_*=\frac{h\tan\theta_w}{(\sigma/\rho_T-1)d_m} \tag{14}$$

where τ_{*c} is the non-dimensional critical shear stress and τ_* is the non-dimensional shear stress.

3.3 Bottom shear stress equations

For a fully developed stony debris flow constitutive equations that have given by Takahashi et al. are described as follows.

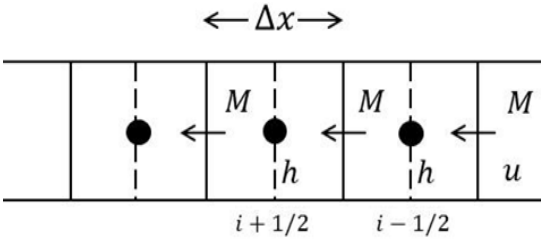

Fig. 7 Definition of arrangement of variables on meshes

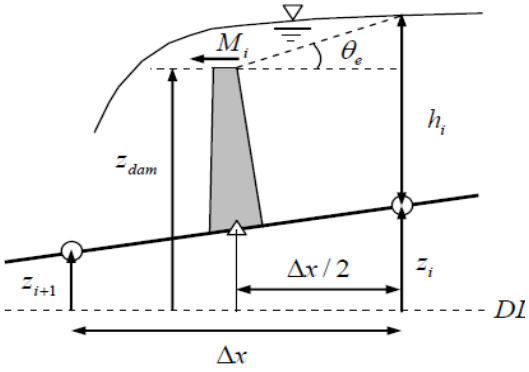

Fig. 8 Definition of the variables and flow surface gradient at closed-type Sabo dam

$$\tau = \tau_y + a_i \sin\alpha_i \left\{ \left(\frac{C_*}{C}\right)^{1/3} - 1 \right\}^{-2} \sigma d_m^2 \left(\frac{\partial u}{\partial z}\right)^2 \quad (15)$$

$$\tau_y = p_s \tan\phi \quad (16)$$

where a_i is experiment constant, α_i is the collisions angle of particle, z is the coordinate perpendicular to the bed and positive upward in the normal direction of flow, p_s is static pressure.

The bottom shear stress for a stony debris flow is derived by substituting the constitutive equations into the momentum conservation equation under a steady and uniform flow conditions;

$$\tau_b = \frac{\rho_T}{8}\left(\frac{d_m}{h}\right)^2 \frac{u|u|}{\{C+(1-C)\rho/\sigma\}\{(C_*/C)^{1/3}-1\}^2} \quad (17)$$

An immature debris flow occurs when C is less than $0.4C_*$ and the bottom shear stress is described as follows;

$$\tau_b = \frac{\rho_T}{0.49}\left(\frac{d_m}{h}\right)^2 u|u| \quad (18)$$

In case of turbulent flow, the Manning's equation is used to determine the bottom shear stress. When C is less than 0.02 as follows;

$$\tau_b = \frac{\rho g n^2 u|u|}{h^{1/3}} \quad (19)$$

where n is Manning resistance coefficient.

3.4 conditions of closed-type sabo dam

The closed-type sabo dam is set at the calculation point of flow discharge per unit width. The effective flow depth, h, at the dam point to

Table 2 Debris flow captured volume

(unit : cm^3)

No.	Lower located sabo dam		Upper located sabo dam		Total	
	Exp	Sim	Exp	Sim	Exp	Sim
Case.A-1	1357.8	1224.5	1978.3	2021.5	3336.1	3246
Case.A-2	1649.8	1352	1912.6	1997.5	3562.4	3349.5
Case.A-3	1635.2	1353.5	1868.8	2041	3504	3394.5
Case.B-1	1843.25	2010.5	2617.05	2383	4460.3	4393.5
Case.B-2	2744.8	2037	2752.1	2342	5496.9	4379
Case.B-3	2117	2123	2802.7	2334.5	4919.7	4457.5

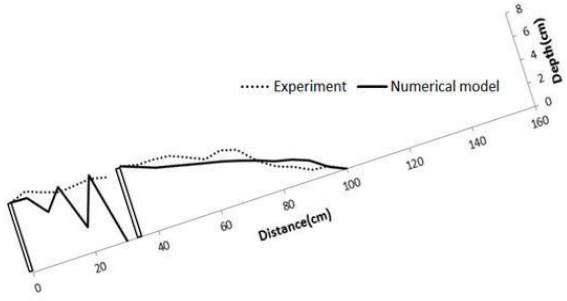

(a) Case.A-1

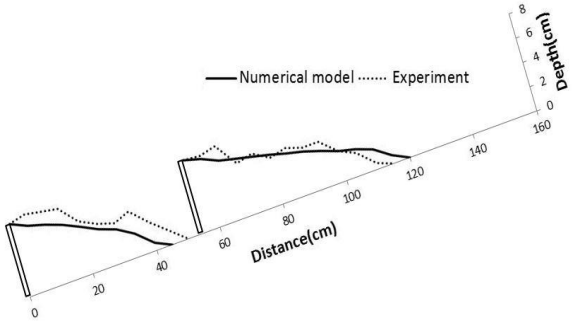

(b) Case.A-2

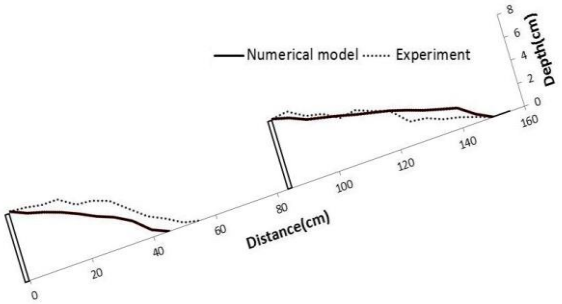

(c) Case.A-3

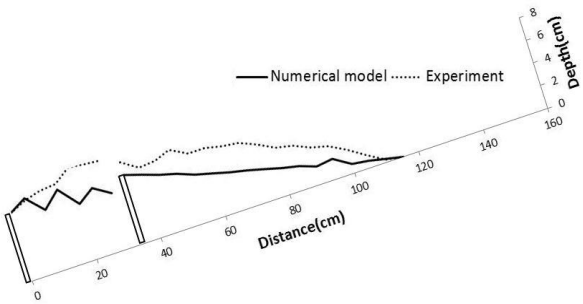

(d) Case.B-1

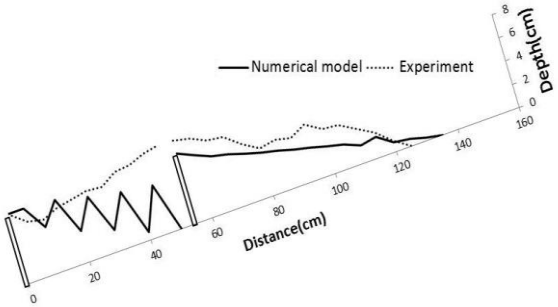

(e) Case.B-2

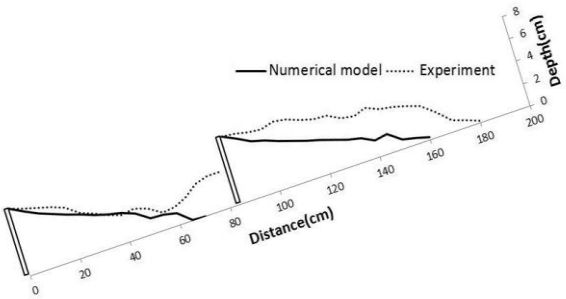

(f) Case.B-3

Fig.9 Final debris flow deposition upstream of sabo dams

calculate the outflow flux and the flow surface gradient, θ_e, are described as follows;

$$h' = \begin{cases} h_i + z_i - z_{dam} & ;(h_i + z_i - z_{dam} > 0) \\ 0 & ;(h_i + z_i - z_{dam} \leq 0) \\ h_i & ; \quad (z_i > z_{dam}) \end{cases} \quad (20)$$

$$\theta_e = \tan^{-1}\left\{\frac{[h_i + z_i - z_{dam}]}{(\Delta x/2)}\right\} \quad (21)$$

The gradient, θ_e', needed to calculate the equilibrium sediment concentration, C_∞, is described as

$$\theta_e' = \tan^{-1}\left\{\frac{[z_i - z_{dam}]}{(\Delta x/2)}\right\} \quad (22)$$

Fig. 7 and Fig. 8 shows the definition of arrangement of variables with the finite difference mesh.

4. Results and discussions

The numerical simulations and experiments were

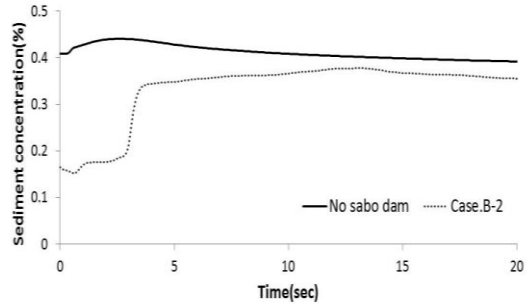

Fig. 10 Sediment concentration at downstream end of flume

performed to investigate capture capacity of sabo dam according to distance of between dam.

Fig. 9 shows the simulated results and experimental results of debris flow deposition upstream of a series of sabo dams. From the figure, simulation results are quite agreement with the experimental results. Because a decrease in distance of between dams is able to increase equilibrium bed slope by upper located sabo dam. However, some discrepancies are found. The equilibrium bed slope of lower located sabo dam is changed by upper located sabo dam. In such case(Case A-1, Case B-1, Case B-2), experimental results shows that upper located sabo dam is almost buried by sediment. In contrast, simulated result shows that sediment deposited form is oscillating. When the debris flow overflows the sabo dam, sediment concentration is decreasing (Fig. 10). This may change the deposition process of lower located sabo dam. Sediment concentration is keep going around 40% without sabo dam. If sabo dam is installed in the channel, sediment concentration is decreasing at forefront of debris flow.

The sediment volume is captured by a series of sabo dams are presented in Table 2. This table show that distance of each dams change, the equilibrium bed slope, θ_e, is changed. Because debris flow deposition form upstream of lower located sabo dam is changed by upper located sabo
am. Case.A-1, Case.B-1, Case.B-2 shows that the changed equilibrium bed slope.

Total debris flow captured volume is the sum of captured volume at lower located sabo dam and upper located sabo dam. All of case, upper located sabo dam captured more sediment than lower located sabo dam. In experimental result, sediment captured volume at upper located sabo dam is accounted for around 55% of the total captured volume. Also, in simulated result, sediment captured volume at upper located sabo dam is accounted for around 56% of the total captured volume.

In this study was evaluated the debris flow captured volume by distance of each sabo dam. The equilibrium bed slope, θ_e is changed by distance of each sabo dam. By considering the depositing processes on lower located sabo dam, more clearly calculated result could be found.

5. Conclusions

This study has shown that debris flow capture capacity by arrangement of sabo dam. As a result, it is shows that a decrease in distance of between dams will increase equilibrium bed slope of lower located sabo dam due to upper located sabo dam. Second, Upper located sabo dam could capture more sediment than lower located sabo dam. Through considering the combination of sabo dams, it is expected to seek further advancements in technical criteria and guidelines. However, it is necessary to modify the mathematical model about changes of overflowed debris flow characteristics.

Acknowledgements

This research is supported by JSPS AA Science Platform Program(Coordinataor: H. Nakagawa) and support of Wakate fund program by Kyoto University Global COE Program(GCOE-ARS).

References

Takahashi, T., Nakagawa H., Harada, T. and Yamashiki, Y. (1992): Routing debris flows with particle segregation, Journal of Hydraulic Engineering, ASCE, Vol. 118, No. 11, pp.1490-1507.

Hunger, O., Evans, S. G., Bovis, M. J. and Hutchinson, J. N. (2001): A review of the classification of landslides of the flow type, Environmen. Eng. Geosci., No.78, pp.359-238.

VanDine, D. F. andBovis, M. (2002): Hstory and goals of

Canadian debris-flow research, Nat. Hazards, Vol. 26(1), pp.67-80.

Honda N., Egashira S. (1997): Prediction of debris flow characteristics in mountain torrents, In Proceedings of 1st International conference on debris-flow Hazards Mitigation, ASCE, pp707-716.

Imran, J., Gary Parker, Jacques Locat and Homa Lee. (2001): 1D numerical model of muddy subaqueous and subaerial debris flows, Journal of Hydraulic Engineering, ASCE, Vol. 127, No. 11, pp.959-968.

Mizuyama, T. andY. Ishikawa. (1988): Technical standard for the measures against debris flow (drift), Technical Meorandum of PWRI, No. 2632.

Johnson, A. M. and McCuen, R. H. (1989): Silt dam design for debris flow mitigation, J. Hydraul. Eng., Vol.115, No.9, pp.1293-1296.

Shrestha, B. B., Nakagawa, H., Kawaike, K. and Baba, Y. (2008): Numerical simulation on Debris-flow deposition and erosion processes upstream of a check dam with experimental verification, Annuals of Disaster Prevention Research Institute, Kyoto University, No.51 B.

Chatwin, S.C., J.W. Schwab andD.N. Swanston. (1994): A guide for management of landslide-prone terrain in the pacific northwest 2nd, Land Management Hand book, No. 18, pp.153-155.

Rabindra Osti, Shinji Egashira. (2008): Method to improve the mitigative effectiveness of a series of check dams against debris flows, Hydrological processes, Vol.22, pp.4986-4996.

Nakagawa, H., Takahashi, T., Satofuka, Y., and Kawaike, K. (2003): Numerical simulation of sediment disasters caused by heavy rainfall in Camuri Grande basin, Venezuela 1999, Proceedings of the 3st Conference on Debris-Flow Hazards Mitigation.: Mechanics, Prediction, and Assessment, pp.671-682.

Takahashi, T., Nakagawa H., Satofuka, Y. and Kawaike, K (2001).: Flood and sediment disasters triggered by 1999 rainfall in Venezuela; A river restoration plan for an alluvial fan, Journal of Natural Disaster Science, Vol.23, pp.65-82.

(Received June 10, 2013)